Characterizing the thermal effects of vegetation on urban surface temperature

Yang, Jinxin; Shi, Qian; Menenti, Massimo; Xie, Yanhua ; Wu, Zhifeng; Xu, Yong; Abbas, Sawaid

DOI
10.1016/j.uclim.2022.101204

Publication date
2022

Document Version
Final published version

Published in
Urban Climate

Urban Climate 44 (2022) 101204

Contents lists available at ScienceDirect

Urban Climate

journal homepage: www.elsevier.com/locate/uclim

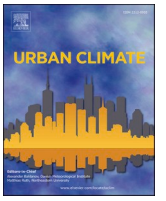

Characterizing the thermal effects of vegetation on urban surface temperature

Jinxin Yang [a], Qian Shi [b], Massimo Menenti [c,d], Yanhua Xie [e], Zhifeng Wu [a,*], Yong Xu [a], Sawaid Abbas [f]

[a] School of Geography and Remote Sensing, Guangzhou University, Guangzhou 510006, China
[b] School of Geography and Planning, Sun Yat-sen University, Guangzhou 510275, China
[c] Faculty of Civil Engineering and Earth Sciences, Delft University of Technology, P. O. Box 5048, 2600 GA Delft, the Netherlands
[d] State Key Laboratory of Remote Sensing Science, Institute of Remote Sensing and Digital Earth, Chinese Academy of Sciences, Beijing 100101, China
[e] Nelson Institute Center for Sustainability and the Global Environment (SAGE), University of Wisconsin-Madison, 1710 University Avenue, Madison, WI 53726, USA
[f] Center for Geographic Information System, University of the Punjab, Lahore, Pakistan.

ARTICLE INFO

Keywords:
Vegetation cooling effects
Urban heat island
Remote sensing

ABSTRACT

Vegetation is important for urban heat mitigation. The cooling intensity of vegetation is affected by background climate and urban design. How to evaluate vegetation cooling efficiency under different climate conditions is still an issue open to discussion. In this study, a normalized indicator of urban vegetation cooling efficiency (NVCE) is proposed as a metric of urban vegetation cooling efficiency applicable and comparable under different climate and urban conditions. When surfaces are only covered by vegetation, the cooling effects should be highest than other pixels at the local climate scale. The difference of surface temperature between the pure vegetation surfaces and surfaces without vegetations ($T_{r,\,b} - T_{r,\,v}$) is the range of the vegetation cooling intensity at the same local climate conditions. Difference between radiometric surface temperature of a mixed pixel and the vegetation temperature within the mixed pixel ($T_{i,\,r} - T_{i,\,v}$) is excess temperature of pixel *i*. The ratio of ($T_{i,\,r} - T_{i,\,v}$) to ($T_{r,\,b} - T_{r,\,v}$) can indicate how much percent of existed excess temperature after vegetation cooling effects for pixel *i* under such local climate condition. Thus, the NVCE is defined as $(T_{i,\,r} - T_{i,\,v})/(T_{r,\,b} - T_{r,\,v})$. Based on the high spatial resolution data, the $T_{i,\,v}$ and $T_{i,\,r}$within each 30 m × 30 m grid are derived to calculate the NVCE and the relationships between NVCE and fractional vegetation cover were studied under different conditions. Results showed that NVCE can reduce the differences caused by background climate in the assessment of vegetation cooling efficiency, i.e. making vegetation cooling efficiency under different climate conditions comparable. The NVCE is also sensitive to the vegetation fraction. When vegetation fraction is smaller than 0.2, the mean value of NVCE is about 0.5 and no obvious change. This means that the vegetation has no obvious cooling effects when vegetation fraction is smaller than 0.2. When the vegetation fraction is higher than 0.2, NVCE decreases linearly with increasing vegetation fraction. When the vegetation fraction is higher than 0.9, NVCE tends to 0. This indicates that 0.2 for vegetation fraction is the threshold of vegetation cooling effects. This study can provide information for evaluating the vegetation cooling efficiency under different

* Corresponding authors.
E-mail addresses: Yangjx11@gzhu.edu.cn (J. Yang), shixi5@mail.sysu.edu.cn (Q. Shi), m.menenti@tudelft.nl (M. Menenti), xie78@wisc.edu (Y. Xie), zfwu@gzhu.edu.cn (Z. Wu), xu1129@gzhu.edu.cn (Y. Xu), sawaid.rsgcrl@pu.edu.pk (S. Abbas).

https://doi.org/10.1016/j.uclim.2022.101204
Received 17 March 2022; Received in revised form 8 May 2022; Accepted 26 May 2022
Available online 11 June 2022

climate and geometric conditions. This study also can provide useful information for urban green infrastructure design and planning, e.g. the vegetation fraction should be higher than 0.2 for urban cooling and the vegetation cooling efficiency can reach maximum when SVF is about 0.5 to 0.6.

1. Introduction

The process of urbanization changes the thermal environment of cities by converting rural surfaces to urban land uses/covers with diverse geometric characteristics. This makes surface energy exchange of urban areas different from rural, resulting in urban air and surface temperatures being higher than rural areas (Oke et al., 2017b; Oke, 1982; Ren et al., 2022). This effect is called urban heat island (UHI) (Oke, 1982; Taha, 1997). Since more and more people live in urban areas (Xu et al., 2021; Yu et al., 2022), monitoring the urban thermal environment and climate is important for urban sustainability and resident health (Ho et al., 2017; Tomlinson et al., 2011; Wei et al., 2021). Urban surface temperature is an important property of the urban thermal environment and remote sensing is an useful tool to observe the urban surface temperature, because it provides frequent and spatially continuous data (Weng, 2009; Peng et al., 2021; Ren et al., 2022; Chen et al., 2022; Zhan et al., 2014).

During the past few decades, numerous studies found that increasing vegetation cover is an effective intervention to mitigate excess heat and to reduce air and surface temperature in urban areas (Weng et al., 2004; Yao et al., 2017; Chen et al., 2006; Yu et al., 2020; Zhou et al., 2016; Zhou et al., 2017; Zhao et al., 2021). Vegetation in urban areas increases the energy used for evapotranspiration (latent heat flux), which reduces the excess energy to be dissipated as sensible heat flux, thus leading to lower air and surface temperature in the urban environment(Cui et al., 2021; Yu et al., 2020). Additionally, urban vegetation may even be critical to prevent extreme urban-rural temperature differences during heat waves (Li et al., 2020). Because of the important effects of vegetation in urban areas, the impacts of vegetation on the urban climate have been investigated in detail using numerical experiments and observations (Holmer et al., 2013; Amiri et al., 2009; Alexander, 2021).

Weng et al. (2004) analyzed the land surface temperature–vegetation abundance relationship in the context of studies on the urban heat island. Results showed that the spatial variability of texture in urban surface temperature (UST) was positively correlated with the normalized difference vegetation index (NDVI) and vegetation fraction. Yuan and Bauer (2007) evaluated impervious surface area and NDVI as potential drivers of surface urban heat island intensity using Landsat imagery. These studies were focused on the effects of the vegetation fraction on the radiometric surface temperature of mixed pixels observed by remote sensing. On the other hand, the vegetation spatial pattern within the urban fabric has a significant impact on both air and surface temperature through complex interactions between vegetation and buildings (Alexander, 2021; Krayenhoff, 2014; Zhou et al., 2011). Trees and buildings shelter each other and both modify their shared radiation, turbulent and thermal environments.

Considering that the vegetation has significant effects on reducing urban surface temperature, Krayenhoff et al. (2021) reviewed the vegetation cooling effects based on numerical simulation studies and defined an index of Vegetation Cooling Effectiveness (VCE) as the ratio of decreased surface temperature to the added vegetation fraction. Vegetation cooling effects are not only related to the vegetation fraction, but also to the background climate conditions and to the spatial distribution of vegetation (Chen et al., 2014; Yu et al., 2020; Yu et al., 2018; Cui et al., 2021). Yu et al. (2018) proposed a cooling effect framework and selected eight typical cities located in Temperate Monsoon Climate (TMC) and Mediterranean Climate (MC) to demonstrate that local climate conditions largely affect the cooling effect of vegetation. Holmer et al. (2013) studied how vegetation, built-up structures and position within the built-up area influenced the nocturnal cooling in the city of Ouagadougou, and results showed that vegetation has different cooling effects under different site-specific conditions. Kuang et al. (2015) analyzed the urban surface temperature of urban areas of Beijing and results showed that the evaporation rate of trees in urban areas is correlated with the texture of the urban fabric. These results show that the vegetation and buildings have complex interactions.

These studies showed that vegetation has significant effects on surface temperature, the impacts of background climate conditions and urban layout on vegetation cooling effects should be considered. Vegetation in urban areas reduces urban surface temperature by evapotranspiration(ET) (Qiu et al., 2013). ET increases with increasing vegetation fraction (Wong et al., 2015) and this helps to cool down urban surface temperature. (Kuang et al., 2015) showed that the heat dissipation efficiency by vegetation, defined as the ratio of latent heat flux to the vegetation fraction, declined with increasing vegetation fraction. ET is not only related to the local vertical gradient of vapor pressure, but is also related to the temperature difference between the vegetation and its surroundings, which triggers advection of sensible heat. Thus, the difference between the surface temperature of vegetation and the surrounding pixels can be used as an indicator of urban vegetation cooling effects. While the difference between vegetation temperature and urban surface temperature is affected by background climate and urban layout. Thus comparing vegetation cooling effects under different background climate and urban layout should consider those factors.

The VCE defined by Krayenhoff et al. (2021) and the heat dissipation efficiency by vegetation defined by (Kuang et al., 2015) do not include these factors, making it incapable of separating climate and vegetation effects on thermal conditions. One reason may be that the high spatial resolution thermal images unavailable to extract the vegetation and surrounding surface temperature. A parsimonious indicator of urban vegetation cooling effects is necessary and it should be evaluated quantitatively under different climate and urban conditions. The abundance and state of vegetation can be characterized by different spectral indices (Gao et al., 2020), e.g. NDVI, which can only detect the presence of vegetation, however, not its thermal effects. Monitoring the vegetation effects on the urban thermal environment is important, thus we need to identify and evaluate a proper indicator of the influence of vegetation, preferably

based on remote sensing observations of the radiometric surface temperature of the heterogeneous urban surface.

Thus, the objectives of this study are: a) to develop an indicator of the vegetation cooling efficiency; b) to evaluate the indicator. In order to reach those objectives, firstly, we proposed a new indicator based on the normalized difference between vegetation temperature and the temperature of mixed pixels to measure the influence of vegetation on the radiometric surface temperature. This difference is normalized to weather/climate and geometric conditions by dividing this difference by its maximum value for each (sub) area. The maximum value is estimated on the basis of image data on samples with full vegetation cover respectively no vegetation. High spatial resolution thermal images were used to obtain the vegetation surface temperature in the heterogeneous mixed pixels to study the cooling effects of urban vegetation. Numerous studies showed that vegetation cooling effects change with the vegetation fraction. Thus, investigating the relationship between NVCE and F_v is a way to evaluate whether the NVCE is applicable and sensitive under a broad range of conditions. Then the high spatial resolution data were degraded to 30 m to obtain the F_v at an easily available spatial resolution, i.e. L8 and L9/OLI and TIRS.

2. Study areas and data

The urban areas of Hong Kong were selected as the study area. Hong Kong is an extremely dense city with high and compact buildings. In order to extract the high accuracy vegetation surface temperature and the vegetation fraction, airborne high spatial resolution (HR) optical and thermal data observed in the urban area of Kowloon (Fig. 1) were used in this study. The thermal data were obtained by the thermal camera FLIR T650sc which was set on a helicopter at the height of 610 m. The spectral coverage of the camera is from 7.5 to 13 μm. In order to analyze the vegetation cooling effects under different background weather conditions, the HR thermal images obtained in daytime on Oct 24, 2017 (autumn) and Jan 14, 2018 (winter) respectively were used in this study. On Oct 24, 2017, the HR thermal data were obtained from about 11:30 (first stripe) to 12:20 (last stripe) in daytime. On Jan 14th 2018, the HR thermal data were obtained from 13:32 to 14:40 in daytime (Fig. 2). In order to obtain the accurate urban surface temperature, the atmospheric temperature and relative humility provided by Hong Kong Observatory were used to correct the atmospheric effects using the FLIR thermal image processing software. Then the material emissivity of each facet type from "The spectral Library of Impervious Urban Materials "(Kotthaus et al., 2014) and the land cover data from high spatial resolution optical data was used to correct for the emissivity. The detailed information about the data observation and processing can be found in Yang et al. (2021b).

The thermal images were acquired by an imaging radiometer onboard a helicopter at very high spatial resolution (HR) with 1 m

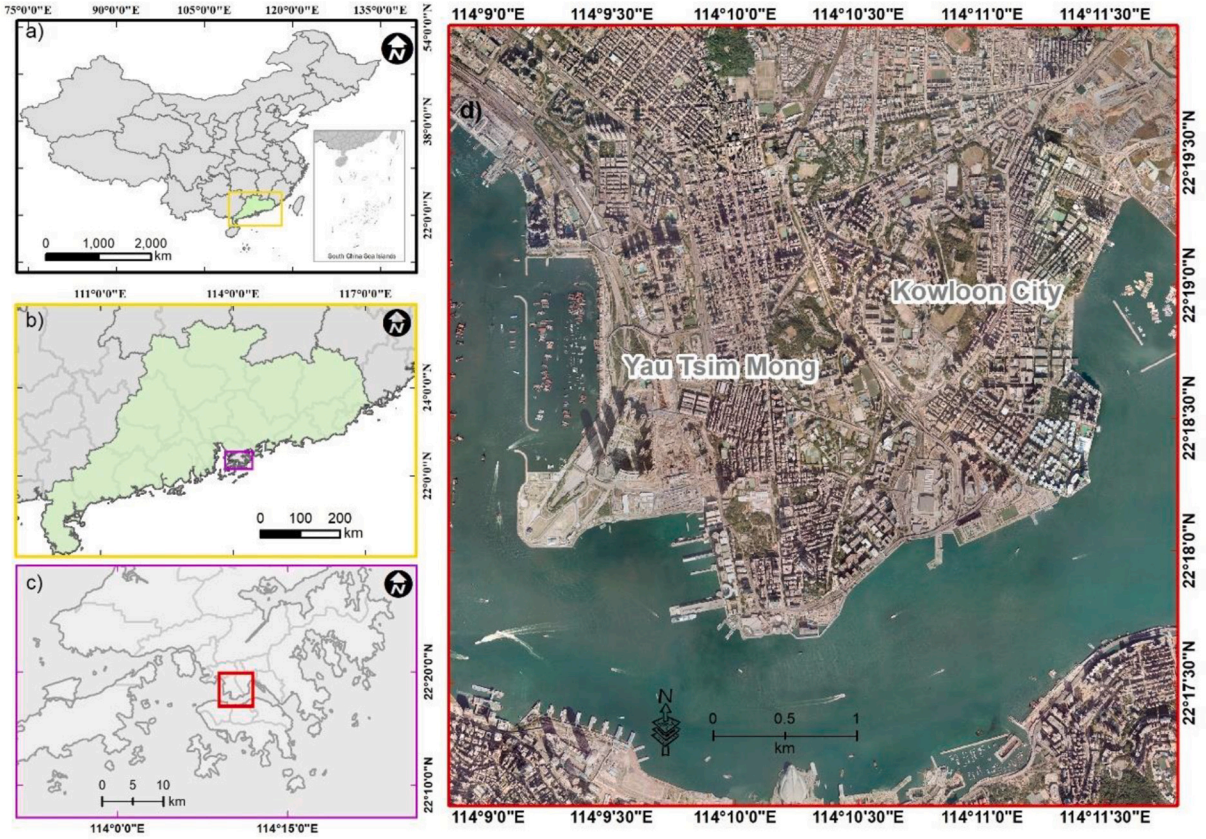

Fig. 1. Study area in this study.

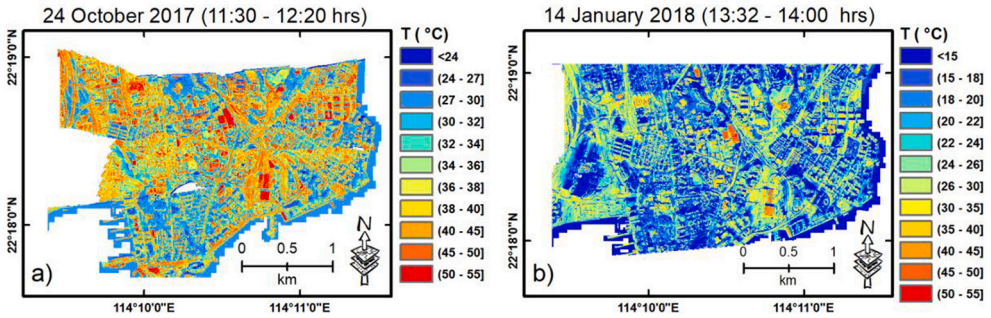

Fig. 2. High resolution thermal images used in this study: a, Oct 24 2017; b, Jan 14 2018.

after processing. The land surface temperature of buildings and vegetation can be obtained detailly. In order to extract the accuracy vegetation cover, multi-spectral high-resolution (0.5 m) data were used to extract the vegetation cover manually in the compact urban areas of Hong Kong (Fig.3). Because the SVF is the main geometric driver of the surface energy balance of urban facets (Oke et al., 2017a), the sky view factor (SVF) at 1 m spatial resolution was used to characterize the urban geometry in this study (Fig. 3). The SVF is calculated from the Digital Surface Model at 1 m spatial resolution of Hong Kong (Lai et al., 2012) and based on the SVF calculation method developed by (Zakšek et al., 2011). More information on SVF can be found in (Yang et al., 2021b; Yang et al., 2015).

3. Methodology

When surfaces are only covered by vegetation, the cooling effects should be highest than other pixels at the local climate scale. The difference of surface temperature between the pure vegetation surfaces and surfaces without vegetations ($T_{r,\,b} - T_{r,\,v}$) is the range of the vegetation cooling intensity at the same local climate conditions. Difference between radiometric surface temperature of a mixed pixel and the vegetation temperature within the mixed pixel ($T_{i,\,r} - T_{i,\,v}$) is the excess temperature of pixel i after vegetation cooling. Considering that the vegetation cooling efficiency changes with the background climate and urban characteristics, a normalized index should be used to represent the vegetation cooling effects under different conditions. To define a metric applicable to the effects of vegetation on the mean surface temperature of mixed pixels, we defined the normalized vegetation cooling efficiency (NVCE) indicator as:

$$NVCE_i = \left(T_{i,r} - T_{i,v}\right) / \left(T_{r,b} - T_{r,v}\right) \tag{1}$$

where $T_{i,\,r}$ is the radiometric surface temperature of mixed pixel i, $T_{i,\,v}$ is the vegetation temperature within the mixed pixel i. $T_{r,\,b}$ is the radiometric surface temperature of built-up pixels without vegetation, $T_{r,\,v}$ is the radiometric surface temperature of vegetation pixels without built-up elements. The value of NVCE approaches zero when the fractional abundance of vegetation within pixel i increases and $T_{i,r} \rightarrow T_{i,v}$. When NVCE is close to 0, the excess temperature is close 0 and the vegetation cooling efficiency reaches maximum.

In order to check whether this indicator is a correct indicator, we correlated NVCE with the vegetation fraction (F_v). The background climate and urban layout can affect the vegetation and urban surface temperature. The indicator NVCE considers the normalized difference between observed urban surface temperature and the local vegetation surface temperature, thus can filter-out effectively the effects of local background climate and urban design conditions, which determine the limiting temperatures $T_{r,b}$ and $T_{r,\,v}$.

T_r in urban areas is heavily affected by urban geometry (Voogt and Oke, 1998). Many geometric parameters affect the urban surface temperature, including building density, height and street aspect ratio (Yang et al., 2020; Yang et al., 2021a). The SVF accounts for the effect of urban geometry on irradiance and net radiation at urban facets. Several studies (Yang et al., 2021a) showed that SVF is the main geometric driver of urban surface temperature. Thus, we binned the observations of F_v and NVCE to investigate this relationship

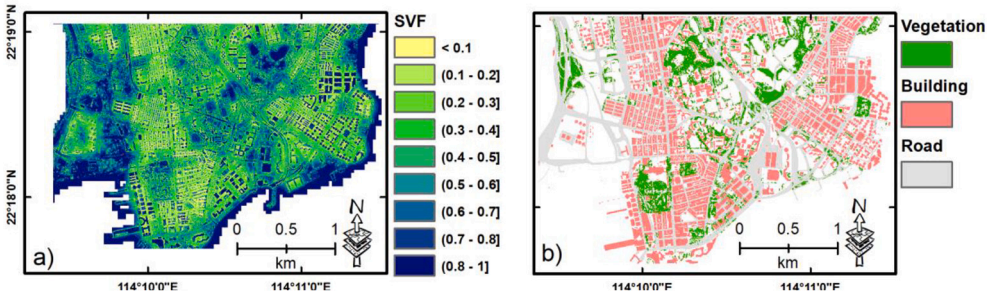

Fig. 3. SVF at 1 m spatial resolution and the vegetation distribution at 0.5 m spatial resolution: a, SVF; b, vegetation.

for different values of SVF, i.e. 0.35,0.45,0.55 and 0.65 with 0.05 range (0.35–0.4, 0.45 to 0.5, 0.55–0.60, 0.65–0.70). It is difficult to retrieve F_v and NVCE of facets where $0 < SVF < 0.25$ because of the blocking by buildings. Observations where $SVF > 0.75$ are very few in compact built-up areas such as Hong Kong. Thus, the SVF bins were set as 0.35–0.40, 0.45–0.50, 0.55–0.60 and 0.65–0.70 in this study.

The vegetation was first extracted from HR optical data at 0.5 m spatial resolution. The objective of this study is to investigate the vegetation cooling efficiency under different conditions and provide an applicable indicator for the cooling efficiency of vegetation. The abundance of vegetation, i.e. Fv, is a widely-used parameter to evaluate the vegetation cooling efficiency(Weng et al., 2004). There are multiple, simple methods to estimate Fv from remote sensing images, most of which requiring multi-spectral image data, specifically capturing the contrast between red and near-infrared reflectance. The latter was actually the limitation in this study, since the high resolution optical images only contain blue, green and red bands, i.e. allowing the classification of the observed target as vegetation or else. Thus, vegetation cover by combining a few full-resolution images was first extracted, and then Fv as the fraction of images classified as vegetation within the sample was estimated at a lower spatial resolution. The high spatial resolution of the thermal images allowed us to retrieve surface temperature at full spatial resolution, then calculate statistics of the vegetation surface temperature at the same spatial resolution as Fv. In order to evaluate the proposed indicator for vegetation cooling efficiency, the indicator should be evaluated at a spatial resolution where Fv is easily available, e.g. Landsat. The spatial resolution of the Landsat thermal bands is 30 m after resampling. Fv at a resolution of 10 m is easily available based on the Sentinel 2 MSI, while high resolution TIR are very rare at 10 m spatial resolution. The linkage between NVCE and Fv provides a first indication of the potential of urban cooling by vegetation in a given urban area, even before undertaking a new study. Thus the HR thermal and optical data were then gridded to 30 m × 30 m.

The vegetation fraction within each 30 m grid was retrieved from 0.5 m high resolution data by calculating the fraction of vegetation pixels within each 30 m grid. More information about the retrieval of the vegetation fractional cover can be found in (Yang et al., 2021b). The vegetation temperature of each grid was retrieved for all facets within the grid at 1 m spatial resolution to calculate the mean value of vegetation temperature ($T_{i,\ v}$). The mean temperature of grids without vegetation was used to calculate $T_{r,\ b}$, while the mean temperature of grids without built-up facets was used to calculate $T_{r,\ v}$. These steps compose the work-flow applied in our study and illustrated in Fig. 4.

4. Results

In order to evaluate whether the NVCE is sensitive to Fv and whether it is an useful metric of the vegetation cooling effects under different background conditions, the relationships between Fv and Tv, Tr-Tv and NVCE were evaluated.

4.1. T_v vs F_v

Vegetation is an important element of urban fabric and vegetation surface temperature is lower than the built-up surface temperature due to evapotranspiration, which is useful for urban heat mitigation. When the *Fv* increases, more vegetation can produce more latent heat fluxes to mitigate excess heat. Thus, the vegetation temperature decreases with the vegetation fraction (Fig. 5), except on Jan 142,018 where SVF is 0.65 (Fig. 5d). And the absolute values of the slopes in the relationship between T_v and F_v on Oct 242,017 were higher than that on Jan 142,018. This is because the evapotranspiration of vegetation increases with the vegetation surface temperature when enough soil moisture is available. Thus, the absolute values of the slope in the relationships between T_v and F_v were

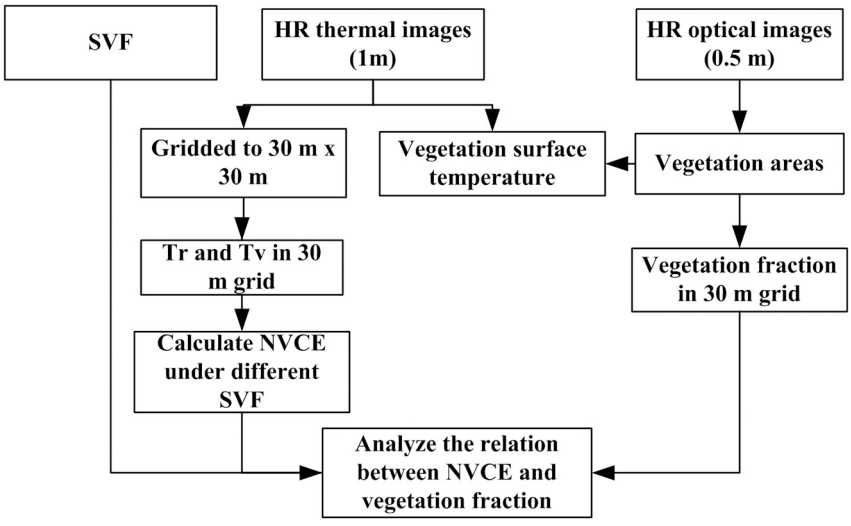

Fig. 4. Work-flow to determine the pixelwise values of the indicator NVCE.

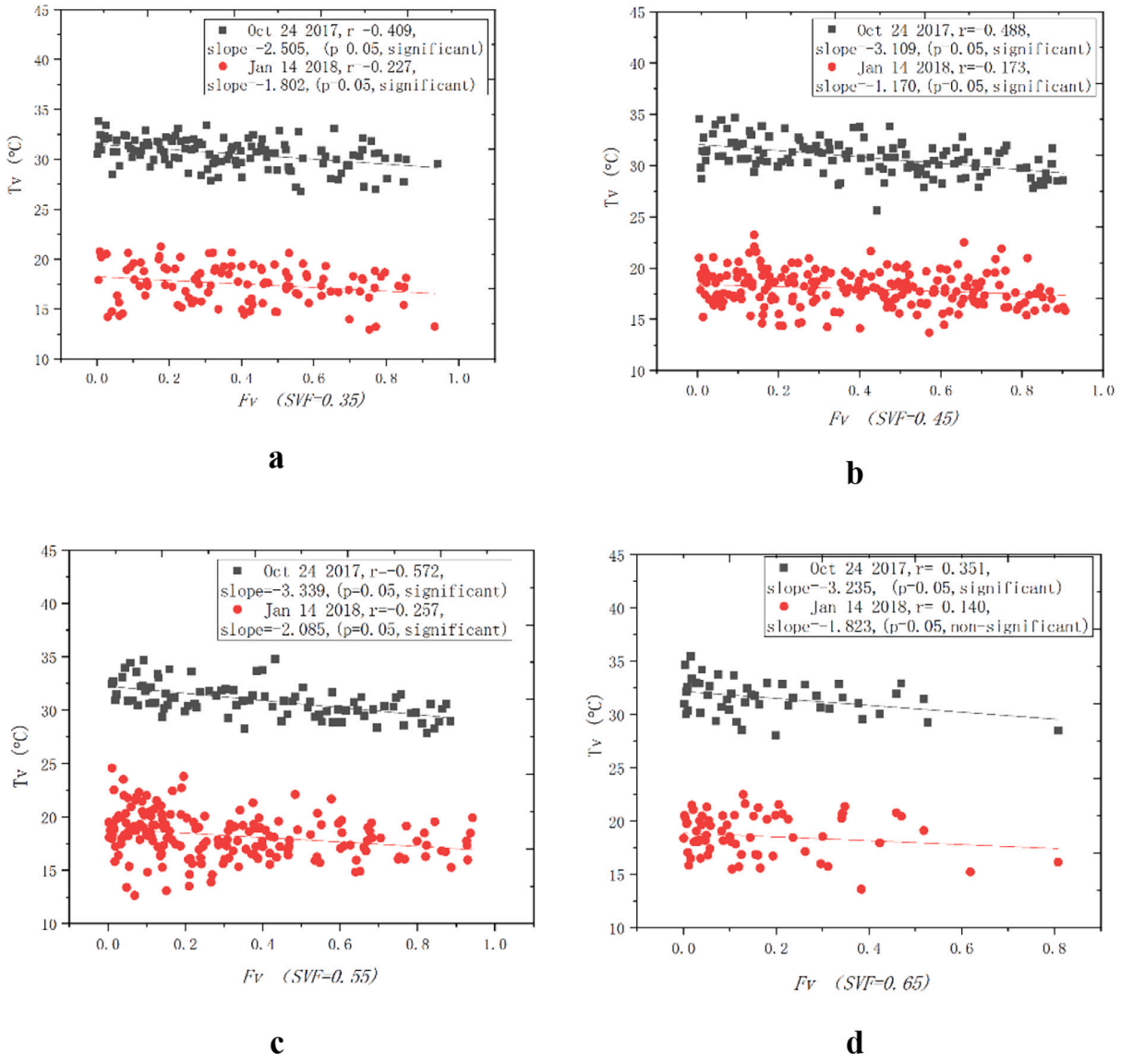

Fig. 5. Vegetation surface temperature changes with F_v at different SVF.

small, indicating a limited sensitivity of T_v to F_v on Jan 142,018. This means the efficiency of vegetation evapotranspiration changes little with the F_v in the winter and the temperature is the crucial factor for the vegetation evapotranspiration.

4.2. T_r-T_v vs F_v

The vegetation in the mixed pixels can cause the decrease of the surface temperature of mixed pixels. T_r-T_v is the surface temperature difference between the vegetation and the surface within the pixel. When the pixel is fully covered by vegetation, T_r-T_v is close to 0 and the vegetation cooling efficiency reaches maximum. When SVF is larger than 0.7, very few observations are available in the compact built-up areas of Kowloon, thus we only studied the relation between T_r-T_v and F_v when SVF is smaller than 0.7. As expected, the T_r-T_v decreases with increasing F_v (Fig. 6). The absolute value of the slope between T_r-T_v and F_v on Oct 242,017 is higher than that on Jan 142,018, and the slope increases with increasing SVF when SVF is smaller than 0.60. When SVF is small and the buildings are compact, the wind flow within the built-up environment is reduced. This affects the vegetation evapotranspiration. Thus, when SVF is higher, the temperature difference between T_r and T_v decreases faster when F_v increases, i.e. when SVF is around 0.5 to 0.6, increasing vegetation fraction has a larger cooling efficiency. When SVF is larger than 0.6, the absolute value of the slope between T_r-T_v and F_v on Oct 242,017 and Jan 142,018 was smaller than that when SVF is smaller than 0.6 (Fig. 6d). One reason is that when the surface is flat, the aerodynamic resistance is higher than in built-up areas. Thus, the latent heat flux may start to decrease when the surface flattens-

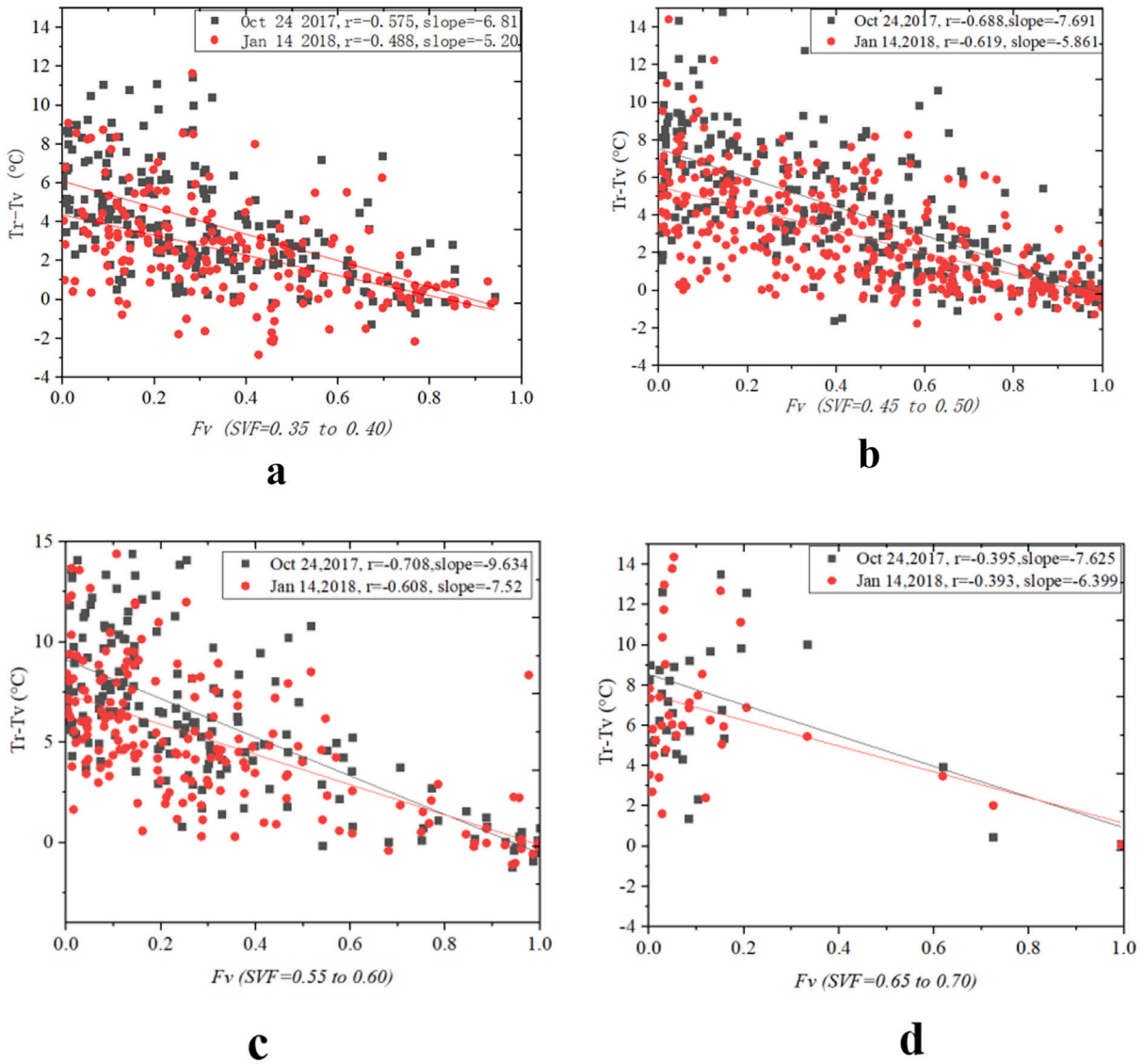

Fig. 6. Temperature difference between Tr and Tv under different conditions: a, SVF =0.35 to 0.40; b, SVF = 0.45 to 0.50; c, SVF = 0.55 to 0.60; d, SVF = 0.65 to 0.70.

out, i.e. SVF > 0.60. Thus, when F_v increases, the temperature difference between T_r and T_v decreases less than that when SVF is between 0.55 and 0.60. These results showed that the threshold values of SVF is about 0.6. When SVF is smaller than 0.6, the vegetation cooling efficiency increase when SVF increases. When SVF is larger than 0.6, the vegetation cooling efficiency will not increase when SVF increases. Comparing with T_v itself, the T_r-T_v is more sensitive to F_v since the absolute values of slopes between T_r-T_v and F_v were much higher than that between T_v and F_v (Table 1). In this sense T_r-T_v is a better indicator for urban vegetation cooling effects than T_v itself.

Table 1
the slopes between different temperature indicators and Fv. (2017 means the Oct 24 2017, 2018 means Jan 14 2018).

	Slopes under different conditions							
	SVF: 0.35–0.40		SVF: 0.45–0.50		SVF:0.55–0.60		SVF:0.65–0.70	
	2017	2018	2017	2018	2017	2018	2017	2018
Tv vs Fv	−2.505	−1.802	−3.109	−1.170	−3.339	−2.085	−3.235	−1.823
Tr-Tv vs Fv	−6.810	−5.200	−7.691	−5.861	−9.634	−7.520	−7.625	−6.399

4.3. NVCE vs F_v

The solar forcing radiation in autumn is higher than in winter, while the difference between T_r and T_v in autumn is higher than in winter and the slope of the relationship between T_r-T_v and F_v is higher than in winter. Additionally, the urban geometry also affects the vegetation and urban surface temperatures. This makes the difference between T_r and T_v to change under different conditions. For example, the maximum reduction in surface temperature at the same vegetation fraction in winter is smaller than in Autumn. The vegetation cooling efficiency was highest in winter. The different climate conditions, e.g. Autumn and winter, make the vegetation cooling effectiveness incomparable and we do not know how the vegetation fraction can reach the maximum effects under certain climate condition. Thus the normalized indicator of urban vegetation cooling effects (NVCE) has the advantage of making comparable the vegetation cooling effectiveness under different background climate and urban layout conditions.

To calculate the NVCE, the reference temperatures are important. Generally, vegetation temperature is relatively homogeneous. Thus, $T_{r,v}$ can directly be estimated as the mean value of pure vegetation pixels. $T_{r,\ b}$ is the maximum temperature of the facets is without vegetation cover. The variability of $T_{r,b}$ is much larger than that of $T_{r,v}$ because of the construction material heterogeneity and geometry (Table 2). How to choose the representative $T_{r,b}$ is important to calculate NVCE. The actual maximum values cannot be used because they appear to be outliers, thus compressing the actual variability of surface temperature in a small range of the full distribution. Accordingly, we proposed two estimates of the maximum temperature, i.e. the mean + 1 std. and the mean + 2 std. to calculate NVCE and impact of these two estimates is compared in Figs. 7 and 8.

In this study, NVCE was calculated using the mean value of $T_{r,b}$ ($\overline{T(r,b)}$), ($\overline{T(r,b)}$+*std*) and ($\overline{T(r,b)}$+2*std*). When $T_{r,b}$ is equal to $\overline{T(r,b)}$, some NVCE values are larger than 1 (Figs. 5 and 6). Results showed that the 6.4% to 12.8% of NVCE values is larger than 1 on Oct 242,017 and 4.7% to 33.7% of NVCE values is larger than 1 on Jan 142,018. Generally, values of NVCE larger than 1 appeared when Fv was smaller than 0.3, if $\overline{T(r,b)}$ is used for $T_{r,b}$.

When Tr,b is taken equal to $\overline{T(r,b)}$ +*std,* very few values of NVCE are larger than 1, and values less than 0 are closer to 0 (Table 3). This means $\overline{T(r,b)}$ +*std* can be a good limiting temperature for Tr,b. When $\overline{T(r,b)}$ +*2std* is used to calculate the NVCE, almost all values of NVCE are smaller than 1. On the other hand, the range of NVCE is relatively narrow when $\overline{T(r,b)}$ +*2std* is used (Table 3).

When $T_{r,b}$ is taken equal to $\overline{T(r,b)}$ +*std,* the absolute values of slopes between NVCE and F_v on Oct 242,017 and Jan 142,018 also increased when SVF was smaller than 0.6 and then decreased when SVF was higher than 0.65. This is similar to the slopes between T_r-T_v vs F_v. From this sense, we can conclude that when SVF is between 0.5 and 0.6, adding the vegetation fraction can reach maximum adding speed of vegetation cooling efficiency in urban areas. The slope values between NVCE and F_v on Oct 242,017 and Jan 142,018 did not indicate significant trends, with the correlation coefficient not significantly different from 0 at $p = 0.05$. Contrariwise, the slopes between T_r-T_v and F_v on Oct 242,017 and Jan 142,018 were clearly different. The absolute values of slopes between T_r-T_v and F_v on Oct 242,017 were higher than that on Jan 142,018. Not all absolute slope values in the relationship between NVCEs and F_v on Oct 242,017 were larger than that on Jan 142,018. This means the NVCE can normalize the background climate effects. This makes the vegetation cooling effects comparable under different climate conditions.

4.4. Comparison between NVCE and T_r - T_v

When we use T_r-T_v to evaluate the vegetation cooling effectiveness, the slope of correlation of T_r-T_v between Oct 242,017 and Jan 142,018 is 0.676 when the vegetation fraction are same. When we use NVCE to evaluate the vegetation cooling effectiveness, the slope of the relationship between NVCE and F_v between Oct 242,017 and Jan 142,018 was 0.850 (Fig. 9). The slope of NVCE between Oct 242,017 and Jan 142,018 was closer to 1 than that of T_r-T_v. This means NVCE can be a better indicator of the vegetation cooling effects under different weather background conditions. Fig. 10 shows the relations between F_v and NVCE on Oct 242,017 and Jan 142,018 and results showed that the NVCE on both dates are very similar to each other. This means NVCE can avoid the background climate conditions for vegetation cooling effect evaluation. In the Fig. 10, the mean value of NVCE is about 0.5 and has no evident change when F_v is smaller than 0.2. When F_v is higher than 0.2, the NVCE decreases fast. When F_v is larger than 0.9, the NVCE is close to 0 and tends to a constant.

Table 2
Mean values of $T_{r,b}$ and $T_{r,v}$ and their *std*.

SVF	Oct 242,017		Jan 142,018	
	$\overline{T_{(r,b)}}$(°C)	$T_{r,v}$ (°C)	$T_{r,\ b}$(°C)	$T_{r,v}$ (°C)
0.35–0.40	37.627	29.605	20.885	16.372
	Std = 3.618		Std = 4.22	Std = 0.89
0.45–0.50	38.439	29.351	20.579	16.612
	Std = 4.012	Std = 2.030	Std = 4.350	Std = 1.292
0.55–0.60	39.947	29.317	24.035	16.988
	Std = 4.417	Std = 1.008	Std = 5.292	Std = 0.691
0.65–0.70	40.230	26.837	24.270	15.879
	Std = 5.537		Std = 5.165	

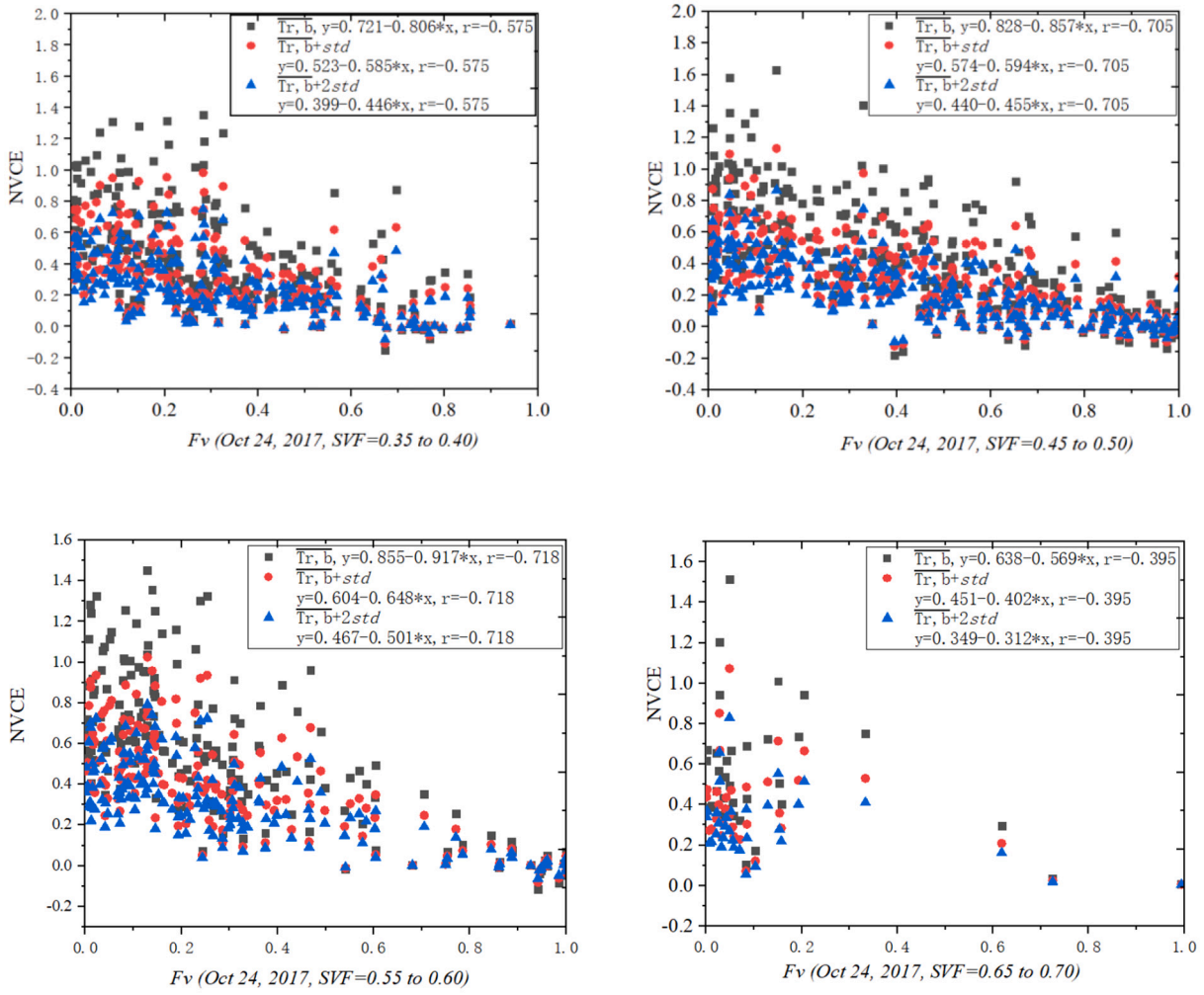

Fig. 7. NVCE of Oct 242,017:a, SVF = 0.35 to 0.40; b, SVF =0.45 to 0.5; c, SVF = 0.55 to 0.60; d, SVF = 0.65 to 0.70.

5. Discussions

Vegetation cooling effectiveness is important for urban vegetation planning and design. Indicators of vegetation cooling effectiveness are generally based on changes in the temperature changes in response to changes in vegetation abundance and distribution in the urban fabric (Krayenhoff et al., 2021). This temperature difference depends on background climate and urban design, as documented by the studies of (Cui et al., 2021; Yu et al., 2018). The maximum temperature difference caused by vegetation, however, is rather different under different background conditions because the maximum evapotranspiration efficiency is different under different background conditions. Thus, the temperature difference is not an univocal indicator to represent the degrade of vegetation cooling effectiveness under the certain background conditions.

In this study, we proposed a normalized vegetation cooling effectiveness indicator named NVCE defined as Eq. (1). The denominator represents the maximum value that this temperature difference can attain under a given climate, i.e. the temperature difference between a built-up patch without vegetation and a patch fully-covered by vegetation under the given climate. The numerator is the real excess temperature after vegetation cooling. Thus NVCE is a metric applicable to indicate the vegetation cooling efficiency under certain background conditions. Results showed that NVCE values in different seasons (Oct 242,017 and Jan 142,018) are closer to each other than values of indicators based on temperature difference only. This means NVCE is a good index for evaluating the vegetation cooling effectiveness of a given configuration of urban space under different background climate conditions. The vegetation cooling indices proposed by Marando et al. (2022)and Krayenhoff et al. (2021) can show how much the temperature change caused by vegetation fraction change is. Under different climate or geometric background conditions, the temperature change caused by a given change in vegetation fraction change is different. This implies the vegetation cooling efficiency cannot be compared for different climate background conditions, for example, vegetation in cold climate of Beijing-tianjin-hebei can mostly cause 1.83 K cooling intensity, while it is 0.0785 k in Urumqi-Changji-Shihezi (Cui et al., 2021). Based only on observed temperature, we cannot directly

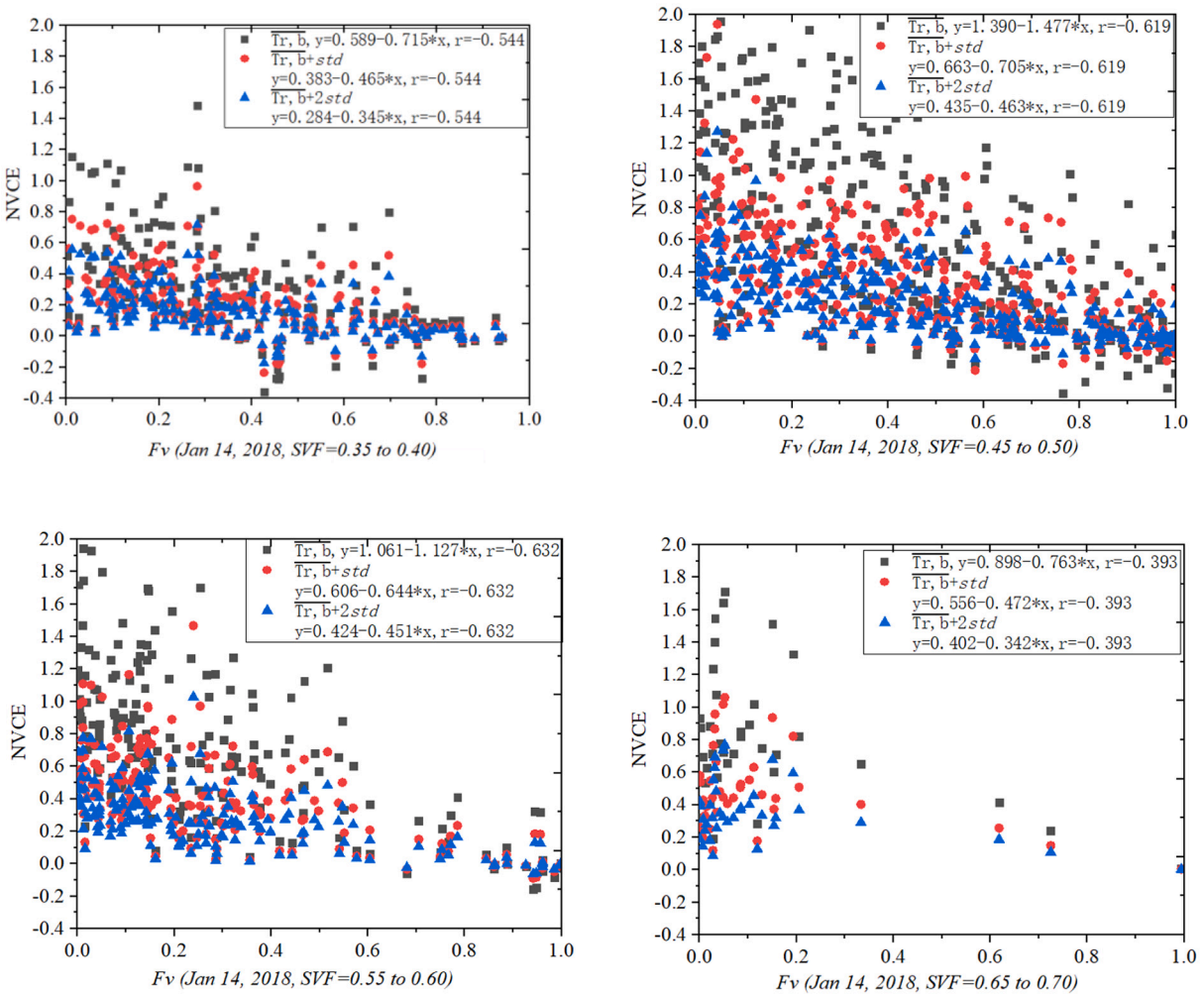

Fig. 8. NVCE on Jan 142,018: a, SVF = 0.35 to 0.40; b, SVF =0.45 to 0.5; c, SVF = 0.55 to 0.60; d, SVF = 0.65 to 0.70.

Table 3
NVCE when different $T_{r,b}$ is used.

		NVCE							
		Oct 242,017				Jan 142,018			
SVF		0.35–0.40	0.45–0.50	0.55–0.60	0.65–0.70	0.35–0.40	0.45–0.50	0.55–0.60	0.65–0.70
$\overline{Tr,b}$	Range	−0.15 to1.35	−0.17 to 1.63	−0.11 to 1.45	0.007 to 1.516	−0.36 to 1.48	−0.44 to 4.06	−0.15 to 2.256	0.007 to 1.7
	NVCE>1	7.6%	6.4%	12.8	9%	4.7%	33.7	26.7	25
	NVCE<0	4.9%	8.3%	3.5%	0	17.5	12.6	6.25	0
$\overline{Tr,b}$+std	Range	−0.109 to 0.983	−0.123 to 1.131	−0.081 to 1.025	0.005 to 1.07	−0.235 to 0.964	−0.211 to 1.940	−0.089 to 1.467	0.004 to 1.060
	NVCE>1	0	0.7%	0.5%	3	0	2.6%	2.8	5.4
	NVCE<0	4.9	8.3%	3.5	0	17.5	12.6	6.25	0
$\overline{Tr,b}$+2*std	Range	−0.084 to 0.749	−0.095 to 0.866	−0.063 to 0.792	0.004 to 0.829	−0.175 to 0.7148	−0.139 to 1.274	−0.063 to 1.02	0.003 to 0.768
	NVCE>1	0	0	0	0	0	0.6%	0.6%	0
	NVCE<0	4.9	8.3%	3.5%	0	17.5	12.6	6.25	0

interpret and compare what degree of vegetation cooling is reached under different weather/climate and geometric conditions. NVCE is a normalized index defined as the ratio of cooling intensity caused by vegetation to the maximum cooling intensity under the same weather/climate and geometric conditions. Thus, NVCE is a universal indicator of the vegetation cooling efficiency, because differences in weather/climate and geometric conditions are normalized by dividing the difference between vegetation and mean pixel

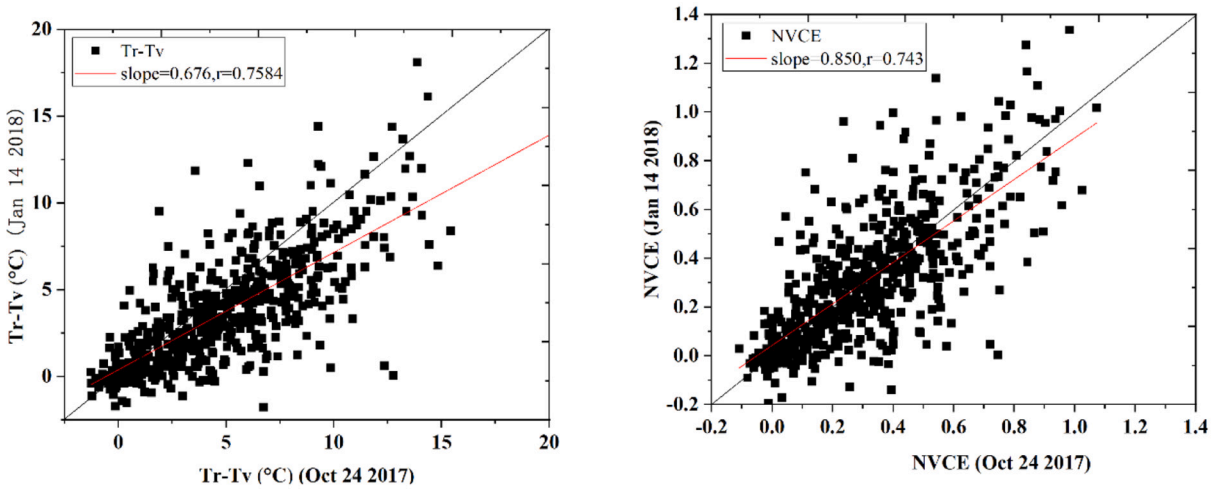

Fig. 9. Relations of Tr-Tv and NVCE between Oct 24 2017 and Jan 14 2018:a, Tr-Tv; b, NVCE.

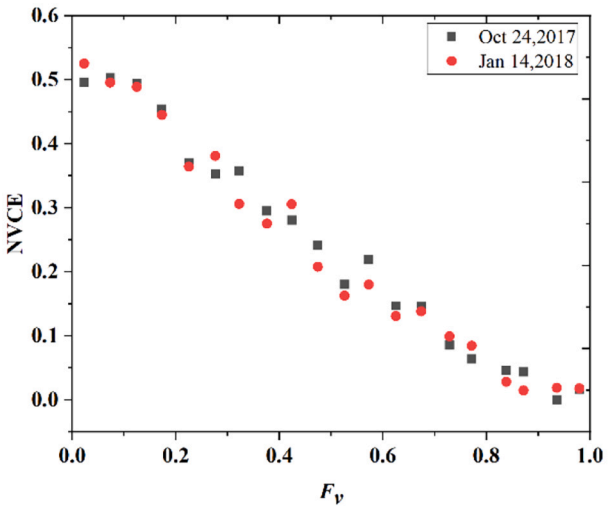

Fig. 10. Relations between NVCE and F_v.

temperature by the (estimated) maximum difference under the same conditions.

The results showed that the NVCE is highest and has no obvious change when vegetation fraction is smaller than 0.2. This means that with Fv $<$ 0.2 urban vegetation does not have any cooling effect. This is similar to the study of (Hou et al., 2014). The study by (Hou et al., 2014) showed that only when vegetation fraction is higher than 0.21, the albedo decreases. This means that when vegetation fraction is higher than 0.2, the irradiance effect can be observed.

The NVCE calculation depends on the reference temperatures of the non-vegetation and pure vegetation pixels. In this study, we recommended that the $\overline{T(r,b)}+std$ should be used to calculate NVCE, with the resulting range of NVCE being close to [0,1]. The surface temperature heterogeneity, however, is different under different local climate zones and the best way to choose the reference temperature $T_{r,b}$ under different conditions requires further studies in the future.

This study also has several limitations. The range of NVCE is from 0 to 1 in this study, while the mean values of NVCE are only about 0.5 when Fv is smaller than 0.2. This means that the standard deviation of NVCE is large. This may be caused by the data used in this study, which were airborne high-resolution thermal data, capturing a very large surface heterogeneity, apparently due to some pixels containing large wall fractions information. The temperature used in this study is the observed radiometric surface temperature, which may also be a limitation. The vegetation cooling effects should consider the temperature of all urban facets. The data were observed in Oct 242,017 and Jan 142,018. These are autumn and winter seasons respectively in Hong Kong. Generally, the vegetation cooling effect is largest in summer. Thus how the NVCE performs in evaluating the vegetation cooling effects in summer season still needs further study in the future.

Additionally, the data used in this study were observed in different seasons and times. Thus, the shadow effects caused by geometry

were different. The sunlit and shadow affect the vegetation transpiration. In this study, the shadow effects have not been considered explicitly, but we have shown that the proposed normalization does normalize for differences in surface temperature due to shadows. The NVCE is then a generic index to evaluate the vegetation cooling efficiency. The mean value of NVCE was not very different at constant Fv on Oct 242,017 and Jan 142,018, notwithstanding the large difference in weather(forcing) conditions. This means that the proposed normalization does correct for differences in forcing when calculating NVCE under different weather/climate and geometric conditions, including shadows.

The NVCE can thus provide a direct indication of the vegetation cooling effectiveness under different weather/climate and geometric conditions. This can help people to evaluate the vegetation cooling effectiveness under different urban design and climate conditions. Only the temperature difference cannot give this information, especially when comparing vegetation cooling effectiveness at different times and seasons. In addition, the transpiration of urban vegetation is related to the temperature difference between vegetation and surrounding surface. NCVE can provide information useful to parameterize urban latent heat flux.

6. Conclusions

Vegetation is an important urban green infrastructure to improve the urban thermal environment. The cooling caused by a given change in vegetation fraction under different forcing conditions is different. This makes useful a normalized metric, such as NVCE, of the vegetation cooling efficiency, which is defined as the ratio of observed temperature difference caused by vegetation to the maximum range of surface temperature difference caused by vegetation under the same climate/weather and geometric conditions. Additionally, we cannot directly interpret the temperature change caused by vegetation to assess the vegetation cooling efficiency. This study proposes a new indicator, i.e. the Normalized Vegetation Cooling Effectiveness (NVCE), to describe the cooling efficiency of vegetation on the urban surface temperature. NVCE is based on the difference between vegetation temperature and the mean radiometric surface temperature of mixed pixels, divided by the maximum possible difference under the same weather/climate and geometric conditions. Results showed that NVCE can indeed reveal the cooling efficiency of vegetation under different weather/climate and geometric conditions. When SVF is about 0.5 to 0.6, the rate of increase in the vegetation cooling effectiveness with increasing vegetation fraction reaches a maximum. In this study, the average values of NVCEs were about 0.5 to 0.6 when the vegetation fraction was close to 0. When the vegetation fraction was close 1, the average values of NVCEs were close to 0. NVCE values on Oct 242,017 and Jan 142,018 were similar at constant F_v: this means NVCE normalizes the vegetation cooling efficiency for differences in weather/climate and geometric conditions, including shadows. Results also showed that when $F_v < 0.2$, the NVCE change is small. When *Fv* is larger than 0.2, the NVCE decreases rapidly with increasing *Fv*. The calculation of *NVCE* is affected by the selections of limiting temperatures and how the limiting temperature should be selected still need more exploration. This study explored how to define a generic vegetation cooling efficiency index to evaluate the urban vegetation cooling and results showed that the NVCE can be used to provide the vegetation cooling efficiency information for different weather/climate and geometric conditions. The NVCE can be used to evaluate the cooling efficiency of urban green infrastructure and makes the vegetation cooling efficiency comparable under different forcing conditions. In addition, the transpiration of urban vegetation is related to the temperature difference between vegetation and surrounding surface. This study can provide information useful to parameterize urban latent heat flux.

Author statement

Yang Jinxin: Conceptualization, Methodology, data process and writing original draft preparation; **Shi Qian**: data process and editing; **Menenti Massimo**: conceptualization review and editing; **Xie Yanhua, Wu Zhifeng and Xu Yong**: Editing; **Sawaid Abbas**: Visualization.

Declaration of Competing Interest

The authors declare no conflict of interest.

Acknowledgement

This work was supported by Grants by National Natural Science Foundation of China (41901283), Guangdong Provincial Natural Science Foundation (2021A1515012567). The authors thank the Hong Kong Planning Department, Hong Kong Lands Department, the Hong Kong Civil Engineering and Development Department, the Hong Kong Observatory and the Hong Kong Government Flying Service for the planning, building GIS, weather and climate, and airborne Lidar data. Massimo Menenti acknowledges the support of grant P10-TIC-6114 by the Junta de Andalucía and the MOST High Level Foreign Expert program (Grant nr. GL20200161002).

References

Alexander, C., 2021. Influence of the proportion, height and proximity of vegetation and buildings on urban land surface temperature. Int. J. Appl. Earth Obs. Geoinf. 95, 102265.

Amiri, R., Weng, Q., Alimohammadi, A., Alavipanah, S.K., 2009. Spatial–temporal dynamics of land surface temperature in relation to fractional vegetation cover and land use/cover in the Tabriz urban area, Iran. Remote Sens. Environ. 113, 2606–2617.

Chen, X.-L., Zhao, H.-M., Li, P.-X., Yin, Z.-Y., 2006. Remote sensing image-based analysis of the relationship between urban heat island and land use/cover changes. Remote Sens. Environ. 104, 133–146.

Chen, A., Yao, X.A., Sun, R., Chen, L., 2014. Effect of urban green patterns on surface urban cool islands and its seasonal variations. Urban For. Urban Green. 13, 646–654.
Chen, Y., Yang, J., Yang, R., Xiao, X., Xia, J., 2022. Contribution of urban functional zones to the spatial distribution of urban thermal environment. Build. Environ. 216, 109000.
Cui, F., Hamdi, R., Yuan, X., He, H., Yang, T., Kuang, W., Termonia, P., De Maeyer, P., 2021. Quantifying the response of surface urban heat island to urban greening in global north megacities. Sci. Total Environ. 801, 149553.
Gao, L., Wang, X., Johnson, B., Tian, Q., Wang, Y., Verrelst, J., Mu, X., Gu, X., 2020. Remote sensing algorithms for estimation of fractional vegetation cover using pure vegetation index values: a review. ISPRS J. Photogramm. Remote Sens. 159, 364–377.
Ho, H.C., Knudby, A., Walker, B., Henderson, S., 2017. Delineation of spatial variability in the temperature-mortality relationship on extremely hot days in greater Vancouver, Canada. Environ. Health Perspect. 125, 66–75.
Holmer, B., Thorsson, S., Lindén, J., 2013. Evening evapotranspirative cooling in relation to vegetation and urban geometry in the city of Ouagadougou, Burkina Faso. Int. J. Climatol. 33, 3089–3105.
Hou, M., Hu, Y., He, Y., 2014. Modifications in vegetation cover and surface albedo during rapid urbanization: a case study from South China. Environ. Earth Sci. 72, 1659–1666.
Kotthaus, S., Smith, T.E.L., Wooster, M.J., Grimmond, C.S.B., 2014. Derivation of an urban materials spectral library through emittance and reflectance spectroscopy. ISPRS J. Photogramm. Remote Sens. 94, 194–212.
Krayenhoff, E. S. (2014) A multi-layer urban canopy model for neighbourhoods with trees.
Krayenhoff, E.S., Broadbent, A.M., Zhao, L., Georgescu, M., Middel, A., Voogt, J.A., Martilli, A., Sailor, D.J., Erell, E., 2021. Cooling hot cities: a systematic and critical review of the numerical modelling literature. Environ. Res. Lett. 16, 053007.
Kuang, W., Dou, Y., Zhang, C., Chi, W., Liu, A., Liu, Y., Zhang, R., Liu, J., 2015. Quantifying the heat flux regulation of metropolitan land use/land cover components by coupling remote sensing modeling with in situ measurement. J. Geophys. Res.-Atmos. 120, 113–130.
Lai, A., So, A.C., Ng, S., Jonas, D., 2012. The territory-wide airborne light detection and ranging survey for the Hong Kong special administrative region. In: The 33RD Asian Conference on Remote Sensing, pp. 26–30.
Li, J., Tam, C.-Y., Tai, A., Lau, N.-C., 2020. Vegetation-heatwave correlations and contrasting energy exchange responses of different vegetation types to summer heatwaves in the northern hemisphere during the 1982–2011 period. Agric. For. Meteorol. 296.
Marando, F., Heris, M.P., Zulian, G., Udías, A., Mentaschi, L., Chrysoulakis, N., Parastatidis, D., Maes, J., 2022. Urban heat island mitigation by green infrastructure in European functional urban areas. Sustain. Cities Soc. 77, 103564.
Oke, T., 1982. The energetic basis of urban heat island. Q. J. R. Meteorol. Soc. 108, 1–24.
Oke, T., Mills, G., Christen, A., Voogt, J., 2017a. Urban Climates.
Oke, T.R., Mills, G., Christen, A., Voogt, J.A., 2017b. Urban Climates.
Peng, J., Dan, Y., Qiao, R., Liu, Y., Dong, J., Wu, J., 2021. How to quantify the cooling effect of urban parks? Linking maximum and accumulation perspectives. Remote Sens. Environ. 252, 112135.
Qiu, G.-Y., Li, H.-Y., Zhang, Q.-T., Chen, W., Liang, X.-J., Li, X.-Z., 2013. Effects of evapotranspiration on mitigation of urban temperature by vegetation and urban agriculture. J. Integr. Agric. 12, 1307–1315.
Ren, J., Yang, J., Zhang, Y., Xiao, X., Xia, J.C., Li, X., Wang, S., 2022. Exploring thermal comfort of urban buildings based on local climate zones. J. Clean. Prod. 340, 130744.
Taha, H., 1997. Urban climates and heat islands: albedo, evapotranspiration, and anthropogenic heat. Energy Build. 25, 99–103.
Tomlinson, C.J., Chapman, L., Thornes, J.E., Baker, C.J., 2011. Including the urban heat island in spatial heat health risk assessment strategies: a case study for Birmingham, UK. Int. J. Health Geogr. 10, 42.
Voogt, J., Oke, T., 1998. Effects of urban surface geometry on remotely-sensed surface temperature. Int. J. Remote Sens. 19, 895–920.
Wei, G., Zhang, Z., Ouyang, X., Shen, Y., Jiang, S., Liu, B., He, B.-J., 2021. Delineating the spatial-temporal variation of air pollution with urbanization in the belt and road initiative area. Environ. Impact Assess. Rev. 91, 106646.
Weng, Q., 2009. Thermal infrared remote sensing for urban climate and environmental studies: methods, applications, and trends. ISPRS J. Photogramm. Remote Sens. 64, 335–344.
Weng, Q., Lu, D., Schubring, J., 2004. Estimation of land surface temperature–vegetation abundance relationship for urban heat island studies. Remote Sens. Environ. 89, 467–483.
Wong, M.S., Yang, J., Nichol, J., Weng, Q., Menenti, M., Chan, P., 2015. Modeling of anthropogenic heat flux using HJ-1B Chinese small satellite image: a study of heterogeneous urbanized areas in Hong Kong. Geosci. Rem. Sens. Lett. IEEE 12, 1466–1470.
Xu, Y., Song, Y., Cai, J., Zhu, H., 2021. Population mapping in China with Tencent social user and remote sensing data. Appl. Geogr. 130, 102450,.
Yang, J., Wong, M.S., Menenti, M., Nichol, J., 2015. Modeling the effective emissivity of the urban canopy using sky view factor. ISPRS J. Photogramm. Remote Sens. 105, 211–219.
Yang, J., Wong, M.S., Ho, H.C., Krayenhoff, E.S., Chan, P.W., Abbas, S., Menenti, M., 2020. A semi-empirical method for estimating complete surface temperature from radiometric surface temperature, a study in Hong Kong city. Remote Sens. Environ. 237, 111540.
Yang, J., Menenti, M., Wu, Z., Wong, M.S., Abbas, S., Xu, Y., Shi, Q., 2021a. Assessing the impact of urban geometry on surface urban heat island using complete and nadir temperatures. Int. J. Climatol. 41, E3219–E3238.
Yang, J., Shi, Q., Menenti, M., Wong, M.S., Wu, Z., Zhao, Q., Abbas, S., Xu, Y., 2021b. Observing the impact of urban morphology and building geometry on thermal environment by high spatial resolution thermal images. Urban Clim. 39, 100937.
Yao, R., Wang, L., Gui, X., Zheng, Y., Zhang, H., Huang, X., 2017. Urbanization effects on vegetation and surface urban Heat Islands in China's Yangtze River basin. Remote Sens. 9, 540.
Yu, Z., Xu, S., Zhang, Y., Jørgensen, G., Vejre, H., 2018. Strong contributions of local background climate to the cooling effect of urban green vegetation. Sci. Rep. 8, 6798.
Yu, Z., Yang, G., Zuo, S., Jørgensen, G., Koga, M., Vejre, H., 2020. Critical review on the cooling effect of urban blue-green space: a threshold-size perspective. Urban For. Urban Green. 49, 126630.
Yu, H., Yang, J., Li, T., Jin, Y., Sun, D., 2022. Morphological and functional polycentric structure assessment of megacity: an integrated approach with spatial distribution and interaction. Sustain. Cities Soc. 80, 103800.
Yuan, F., Bauer, M.E., 2007. Comparison of impervious surface area and normalized difference vegetation index as indicators of surface urban heat island effects in Landsat imagery. Remote Sens. Environ. 106, 375–386.
Zakšek, K., Oštir, K., Kokalj, Ž., 2011. Sky-view factor as a relief visualization technique. Remote Sens. 3, 398–415.
Zhan, W., Ju, W., Hai, S., Ferguson, G., Quan, J., Tang, C., Guo, Z., Kong, F., 2014. Satellite-derived subsurface urban Heat Island. Environ. Sci. Technol. 48, 12134–12140.
Zhao, Z., Sharifi, A., Dong, X., Shen, L., He, B.-J., 2021. Spatial variability and temporal heterogeneity of surface urban Heat Island patterns and the suitability of local climate zones for land surface temperature characterization. Remote Sens. 13, 4338.
Zhou, W., Huang, G., Cadenasso, M.L., 2011. Does spatial configuration matter? Understanding the effects of land cover pattern on land surface temperature in urban landscapes. Landsc. Urban Plan. 102, 54–63.
Zhou, D., Liangxia, Z., Dan, L., Dian, H., Chao, Z., 2016. Climate–vegetation control on the diurnal and seasonal variations of surface urban heat islands in China. Environ. Res. Lett. 11, 074009.
Zhou, W., Wang, J., Cadenasso, M., 2017. Effects of the spatial configuration of trees on urban heat mitigation: a comparative study. Remote Sens. Environ. 195.